Theor Chem Acc (2010) 125:365–373
DOI 10.1007/s00214-009-0632-y

REGULAR ARTICLE

Excitation of the M intermediates of wild-type bacteriorhodopsin and mutant D96N: temperature dependence of absorbance, electric responses and proton movements

Rudolf Tóth-Boconádi · Andras Dér · Stefka G. Taneva · Lajos Keszthelyi

Received: 4 February 2009 / Accepted: 30 August 2009 / Published online: 19 September 2009

Abstract The simplest proton pump known in biological systems, bacteriorhodopsin (bR), is the first ion-transporting membrane protein, the function of which can be described at the atomic level, with the aid of molecular dynamics calculations. To get additional experimental support for the proposed atomic level description of the function of bR, we studied a quasi-stable state of the protein molecule, the so-called M intermediate that plays a crucial role in the proton pumping process. The temperature dependence of the light-induced events occurring in the photocycle of wild-type bacteriorhodopsin and its mutant D96N were followed in detail. Absorbance changes, electric signals generated by charge motion inside the protein, and movement of protons in the protein solution interface either forward (proton release due to excitation of bR) or backward (uptake of protons due to the M excitation: "back-take") were monitored. The obtained Arrhenius parameters indicate that the proton back-take is triggered by charge rearrangements in the protein similar to the proton release triggered by those during the L → M transition. The time necessary for proton back-take determines the reconstitution time of the bR ground state. The data are expected to be used in theoretical modeling of the bR function. Based on these results, a more detailed photocycle model is established to describe the proton pumping mechanism, implying a formal principle ("domino model") that is expected to hold also for other charge transfer proteins.

Keywords Purple membrane · Orientation · Photocycle · Charge motion · Buffer effect · Proton back-take · Domino model

Dedicated to Professor Sandor Suhai on the occasion of his 65th birthday and published as part of the Suhai Festschrift Issue.

R. Tóth-Boconádi · A. Dér (✉) · L. Keszthelyi
Institute of Biophysics, Biological Research Centre, Hungarian Academy of Sciences, P. O. B. 521, 6701 Szeged, Hungary
e-mail: derandra@freemail.hu

S. G. Taneva
Unidad de Biofísica y Departamento de Bioquímica y Biología Molecular, Universidad del País Vasco, 48080 Bilbao, Spain

L. Keszthelyi
KFKI Research Institute for Particle and Nuclear Physics, Hungarian Academy of Sciences, P.O.B. 49 1525, Budapest, Hungary

1 Introduction

Bacteriorhodopsin (bR) molecules in the cell membrane of *Halobacterium salinarum* transport protons from the cytoplasm to the external medium. bR is considered as a paradigm for ion pumps and also for the 7-helix receptor family. It is the first ion-transporting membrane protein, the function of which can be described at the atomic level, purely by physical methods. Absorption kinetic experiments revealed a cyclic reaction scheme associated with the function of bR (the "photocycle"), with the ground state (BR) and six quasi-stable intermediates labeled J, K, L, M, N and O, conventionally characterized by their absorption spectra [1–3] (Fig. 1). Note that, similar to the ground state, the intermediates are also sensitive to light [3–14].

The early steps of the bR proton transport process (until the formation of the M intermediate) are experimentally well characterized and have also been modeled by molecular dynamics simulations [e.g., 15, 16]. Especially the proton transfer step accompanying the L–M transition was thoroughly investigated by theoretical (QM–MM)

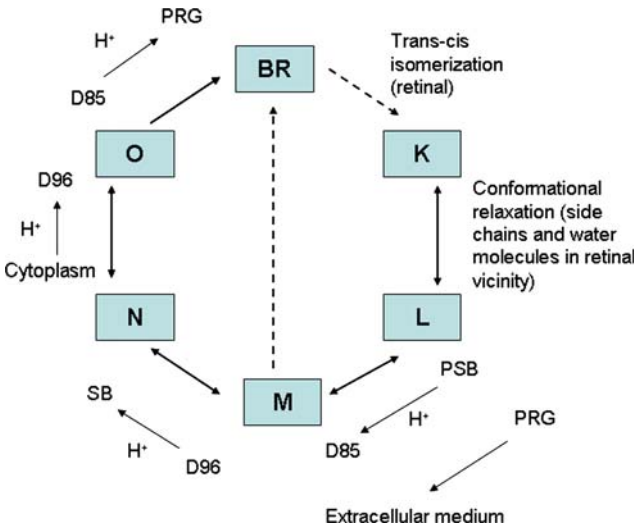

Fig. 1 Simplified scheme of the bacteriorhodopsin photocycle. The letters *K*, *L*, *M*, *N* and *O* denote quasistable conformers (intermediates), while BR stands for the ground state bR. The *dashed lines* indicate light-induced transitions (orange light excites BR, while blue light excites M), while the *solid lines* represent thermally driven ones. The main molecular events are shown aside the relevant transition. *PSB* and *SB* stand for protonated and unprotonated Schiff base, respectively, while *PRG* denotes the proton release group

methods, based on the available experimental data [17]. Concerning the second proton transfer step, when the protein releases a proton to the extracellular side, however, there are still some crucial open questions, despite the considerable amount of information accumulated during the past years [18–20]. The problem is that the process is rather complex, involving a proton release cluster of amino acid side chains and water molecules. While FTIR experiments [20] identify a cluster of water molecules as the proton release group (PRG), according to a recent QM/MM study, a pair of conserved glutamate residues (Glu194/204) bonded by a delocalized proton is the PRG [21].

To reach a consensus and to check the validity of existing models, it appears necessary to include additional experimental information (perform additional experiments) in the analysis, independent of the existing spectroscopic and X-ray data, which alone have not been able to definitively answer this question.

The protein electric response signals (PERS) measured on photoexcitation of bR carry direct information of the proton transport process, and can be used as excellent probes of molecular models, which attempt to describe bR function [5, 21, 22]. PERS can be interpreted as a result of intramolecular electric currents accompanying charge rearrangements inside the protein. A careful evaluation of electric signals yields molecular dipole moment changes associated with reactions in the photocycle [5]. However, based on kinetic arguments, contributions of conformational changes in the protein to the measured experimental parameters cannot always be distinguished and separated from those of the actual proton transfer process. Indeed, a process may be concerted, with the two steps occurring concurrently, rather than being a two-step process. To unravel this problem, we decided to perform a series of studies using flash excitation of the intermediates. Detailed studies of PERS from L excitation have been used to test X-ray structures of the intermediates [23–27], as recently published [12].

The M intermediate, appearing in the microsecond time range with an absorption maximum of 410 nm, has a long lifetime (8 ms in wild-type bR (WTbR) and about 1 s in mutant D96N at room temperature). When excited with blue light, the photocycle is short-circuited: the molecules return directly to the ground state, without pumping (Fig. 1; note that in several kinetic studies, two M intermediates are distinguished (M1 and M2), which are assigned to the protonated or deprotonated states of the PRG. As under our measuring conditions, both of the M intermediates are accumulated, the subsequent excitation by blue flash affects both M intermediates. Hence, unless we specify them, M without indices refers to both of the M intermediates). During this process, bR returns to the ground state without pumping [3, 6–10]. This means that in the reverse direction, the same rearrangements in the molecule should take place in the opposite direction, as in the forward process (BR to M), except that their order and kinetics may be different. On studying the electric signal associated with this process, three components were found: a fast negative one (not resolved in the measurements) [7–10], a positive one with a lifetime of about 30 μs, and a negative one with a lifetime of 600–700 μs [28].

Taking into account recent structural data [27], the first component was assigned mainly to proton uptake by the retinal Schiff base from the Asp85 residue, while the second and third components were tentatively attributed to protein conformational changes in the vicinity of the retinal and in the PRG, respectively. The slowest component was established to reflect charge rearrangements associated with proton uptake by the protein from the bulk [28, 29].

In this paper, we report data on the temperature dependence of PERS, proton uptake (in the following: "back-take") and absorption changes due to M excitation ("M cycle") of wild-type bacteriorhodopsin (WTbR) and its mutant D96N. The results are used to characterize the intramolecular events associated with the proton back-take process of the M cycle. Important implications to the "forward" (proton pumping) photocycle of bR are also discussed.

2 Experimental

Purple membranes containing WTbR were separated from *Halobacterium salinarum* strain R_1M_1; the strain L-33

containing mutant D96N was supplied by J. K. Lanyi. The membrane fragments were oriented and immobilized in polyacrylamide gel as described in Ref. [30]. Slabs measuring $1.6 \times 1.6 \times 0.18$ cm^3 were cut and soaked in a solution (100 cm^3 containing 50 μM $CaCl_2$, 1 mM NaCl at pH 7.5) for overnight, at least, and placed in the same solution into cuvettes.

The sample containing WTbR was flashed by two lasers: a frequency-doubled NdYAG laser 530 nm (Surelite I-10, Continuum) and an excimer laser-driven dye laser (Lambda Physik, EMG 101 MSC, Göttingen, Germany) with dye LC4090 DPS giving 406 nm flash. The NdYAG laser provided the first flash producing the M population and the excimer laser the second**.** A home-made time generator controlled the delay between flashes.

In the case of mutant D96N, substantial M population was produced with quasi-continuous illumination (quasi-continuous means continuous illumination for 2–4 s) with light from a 200-W tungsten lamp filtered for wavelengths above 500 nm. The *M* concentration (M_{CC}) in both cases was determined from the absorbance at 400 nm, measured with a light-emitting diode (Roithner M3L1-HP30, Vienna, Austria) and using the absorption coefficients from Ref. [31]. In the case of WTbR, the blue flash was timed at 200–500 μs after the first flash depending on temperature near to maximal *M* concentration, while for the mutant D96N at 20 ms after the background light was switched off. This way, 23–25 and 65–70% of BR, respectively, was driven to M at temperatures between 5 and 31 °C.

For measuring the proton release and uptake by the protein, in a series of experiments, pH-sensitive dyes were added to the sample. To measure proton uptake after M excitation, 20 μM fluorescein was added to the suspension containing WTbR (we note that blue light needed to excite M decomposes the usually applied proton indicator dye pyranine, and therefore it is not suitable for such measurements). We monitored proton release for 530-nm excitation in the case of D96N using pyranine in solution. The measuring light for fluorescein- and pyranine-containing samples was supplied by diodes emitting at 490 or 450 nm (Roithner LED490-03U, LED450-03U, Vienna, Austria). As an alternative method, the contribution of special buffers, glycyl-glycine (GG) or bis–tris propane (BTP) added to the sample (final concentration: 5 and 1 mM, respectively), to the electric signals was used to monitor proton release and uptake processes [32].

The electric responses were detected using platinized Pt electrodes immersed into the solution and amplified by a home-made current amplifier based on a Burr-Brown 3554 operational amplifier with band width set to 300 kHz. The monitoring light for absorption measurements was registered with a photomultiplier. The signals were digitized and averaged by computer-controlled transient recorder LeCroy 9310L (LeCroy Corp. Geneva, Switzerland) with 10,000 channels.

2.1 Evaluation of the electric signals

The main problem of studying absorbance changes and PERS of a given intermediate is the separation of the contribution due to the unavoidable excitation of the residual ground state and other intermediates (residual means the fraction not excited with the first flash or with the quasi-continuous light). In our case, a plausible assumption is that the overwhelming part of the signal generated by the blue light (406 nm) can be assigned to excitation of the M state and the residual ground state only (as known from, e.g., flash spectroscopic measurements [31], the other intermediates have relatively small extinction coefficients in the blue, and also very small concentrations). After determining the *M* concentration as mentioned above (M_{CC}), the fraction of excited residual ground state (*P*) was determined as detailed in [28]. Briefly, the used thin sample (absorbance at 570 nm $\approx$ 0.3) allowed a linear function to determine *P* as

$$P = \frac{(1 - M_{CC}) \times \varepsilon_{BR}}{M_{CC} \times \varepsilon_{M} + (1 - M_{CC}) \times \varepsilon_{BR}} \quad (1)$$

where ε_{BR} and ε_{M} are the absorption coefficients for BR and M at 406 nm [31]. The value of *P* for WTbR was 40–45%, while for D96N 8–10%. Traces registered for blue flash only were multiplied with factor *P* and subtracted from those registered in the presence of M intermediates.

To analyze the kinetics of the signals, exponentials were fitted to the curves extracted by the above method. Since the components were of distinct time constants and assigned to separate molecular events [28, 29], we chose a model-independent approach, where directly the temperature dependence of the component signals was analyzed. As shown earlier (e.g., in [32, 33]), this is a satisfactory approximation for the description of the bR photocycle in the time regime investigated in this study, and a well-defined physical meaning can be assigned to the derived Arrhenius parameters (even if the component reflects a multiple set of molecular events, the calculated parameters can be related to rate-limiting conformational changes or dominant transitions).

3 Results

3.1 Wild-type bacteriorhodopsin (WTbR)

As mentioned in "Evaluation of the electric signals", we had to determine M_{CC} first. Figure 2 shows the change of absorbance at 400 nm excited with green flash, without and

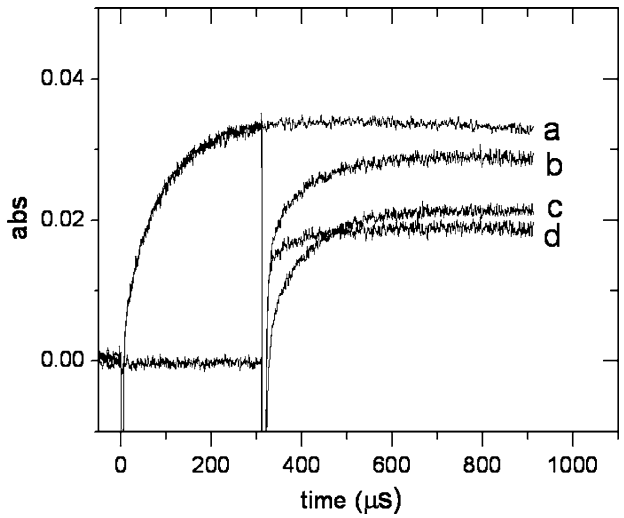

Fig. 2 Wild-type bacteriorhodopsin. Changes of absorbance at 400 nm for *a* the first laser flash (530 nm), *b* for two flashes (second the blue flash 406 nm), *c* for the blue flash, *d* trace *b* − P × trace *c*), i. e., the remaining change after correction for the ground state component excited by the blue flash. Gel sample, solution 1 mM NaCl, 50 μm $CaCl_2$, temperature 21 °C

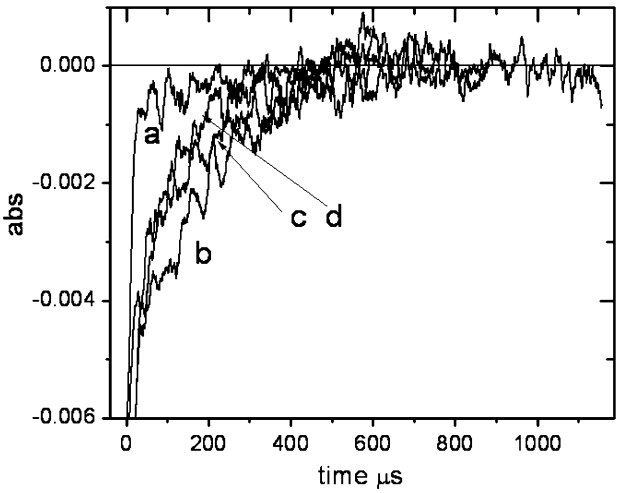

Fig. 3 Wild-type bacteriorhodopsin. Changes of absorbance at 400 nm connected to the excitation of M intermediate. *a–d* corresponds to 7, 14, 21, 28 °C. Data calculated from data similar to those in Fig. 2 as detailed in the text

Table 1 Wild-type bacteriorhodopsin

Component	ΔH kJ/mol	ΔS kJ/mol.deg	τ at 28 °C (μs)
Mrisegreen ill.	56.0 ± 1.8	+0.030 ± 0.004	43.8 ± 0.4
Mriseblue ill.	57.0 ± 1.7	+0.030 ± 0.005	37.1 ± 0.3
Mbackopt	40.8 ± 1.9	−0.033 ± 0.002	55.5 ± 1.6

Arrhenius parameters of the rise of absorbance change due to excitation of M intermediate with green (530 nm) and blue (406 nm) flash, and for the absorbance change due to the M cycle (*Mbackopt*)

with the blue flash (traces *a, b*). It contains the absorbance change for the blue alone (trace *c*), to correct trace *b* for the contribution of the ground state excitation. The blue flashes were always timed at the maximum of the M determined by the rise-time of the traces (*Mrise*). M_{CC} was determined from the absorbance at the time of the blue flash from trace *b* and then the factor *P* from Eq. 1. Trace *d,* representing the real effect of outcome of M excitation, was constructed by subtracting $P \times c$ from *b*. Trace *d* should be strictly parallel to trace *a* if there is no absorbance change due to the M excitation. This absorbance change, in addition to the abrupt fall of M absorbance, appeared by subtracting $F \times a$ from trace *d*, where *F* was taken as the ratio of trace *d* to trace *a* at the very end of the time scale. By performing these calculations with data at four temperatures we got the results presented in Fig. 3. We could refer to these data as optical part of the M cycle. Arrhenius parameters were calculated from two such series and their average presented in Table 1 (*Mbackopt*). In addition, we fitted the *Mrise* traces for the green and blue flashes at the four temperatures and determined the corresponding Arrhenius parameters. These are also listed in Table 1.

The time behavior of proton release is normally recorded with proton-sensitive dyes, generally with pyranine. In this case, however, the proton back-take for blue flash was recorded with fluorescein that is not sensitive to the exciting light of 406 nm. Traces with green, blue and green plus blue flashes (blue flash at 200 μs) were taken with and without fluorescein at 490 nm, and differences between these traces were calculated. For the sake of simplicity, in Fig. 4, we show the fluorescein signal for the green plus blue flash (*a*) and the sum of the two corrections: the green signal multiplied with $1 - P$, the blue signal with P (*b*). The difference, trace *a* − trace *b* = trace *c*, describes the proton back-take (Fig. 4). The lifetime of back-take is 258 ± 6 μs in this case.

This type of measurement, nevertheless, is complicated (many subtractions are needed and the temperature dependence of the answer of fluorescein has to be determined); therefore, we did not follow the temperature dependence of proton back-take with fluorescein, but turned to the much simpler buffer method. As we have already demonstrated, the difference of traces with and without GG buffer coincides with the proton release and renders more information about its time behavior compared with that from proton-sensitive dyes [32, 33].

In Fig. 5a–c, we show traces obtained at 21 °C (*a*) without and (*b*) with GG. Figure 5a depicts PERS for the green flash. We note that the large, fast negative signals, well known from the previous studies [7], are truncated. The GG signals have two time constants representing the real time course of proton release, while the dye signal provides integral of the time course. Determination of the

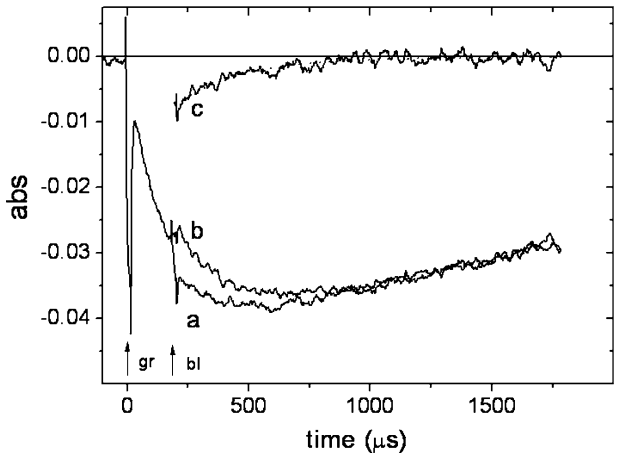

Fig. 4 Wild-type bacteriorhodopsin. Changes of absorbance at 490 nm due to proton indicator dye fluorescein that monitor the presence of protons in solution. Trace *a* corresponds to protons due to green and blue flashes. Traces *b* and *c* are explained in the text. Solution: 100 μM bacteriorhodopsin, 100 μM fluorescein, 160 mM KCl, pH 7, temperature 24 °C

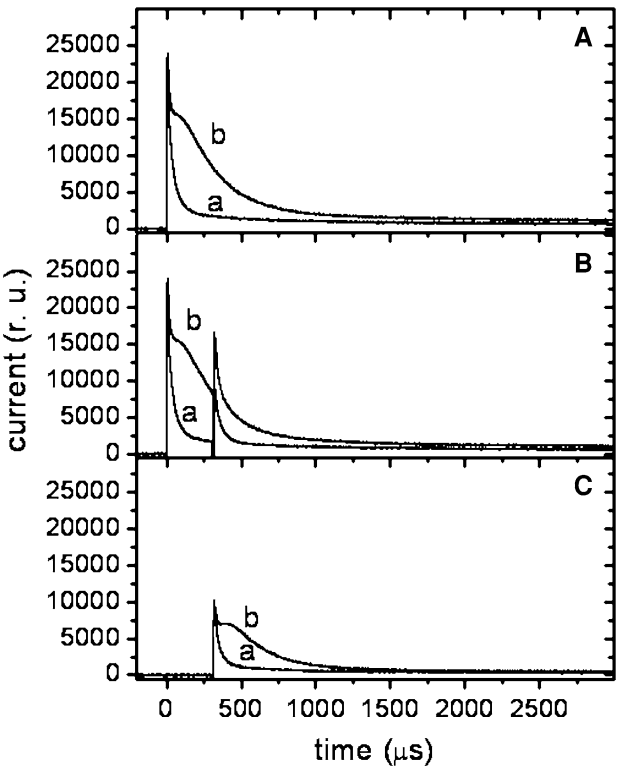

Fig. 5 Wild-type bacteriorhodopsin. Protein electric response signals (**a**) for green flash (530 nm) at zero time, (**b**) for green and blue flash (406 nm) at 300 μs, (**c**) only for blue flash at 300 μs. In the *panels* traces *a* without and *b* with glycyl-glycine. Gel samples, solution 1 mM NaCl, 50 μm $CaCl_2$, or 50 μm $CaCl_2$ and 5 mM glycyl-glycine, temperature 21 C°

real time course (i.e., the short-lived first component) necessitates extremely careful measurements with dyes [34]. In Fig. 5b we see traces representing the event when

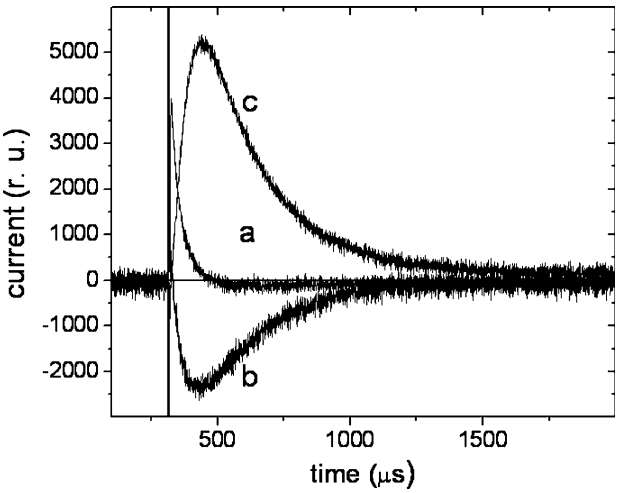

Fig. 6 Wild-type bacteriorhodopsin. *Mback a* and *Pback b*, signals calculated from traces in Fig. 4. *c Pforward* signal for blue flash

the green flash was followed at M_{CC} maximum (300 μs) by a blue flash. Figure 5c contains similar traces, when only the blue flash illuminated the sample at 300 μs. All these traces are necessary for the determination of the time course of the electric signal due to M excitation (*Mbackelec)* and of proton back-take (*Pback*).

Mbackelec was calculated as described above in the case of fluorescein signal, i.e., trace *a* from Fig. 5a was multiplied with $1 - P$ from 300 μs, representing the remaining part of PERS after M excitation, and trace *a* from Fig. 5c with *P*, representing PERS due to the excitation of the residual ground state with blue flash. Subtracting these two traces from trace *a* in Fig. 5b, we obtained *Mbackelec* as shown in Fig. 6 (the traces do not include the first fast negative component of the *Mbackelec* signal).

Our aim was to study the two μs components of *Mbackelec*, consequently the ns range covered in [9] was not taken into account.

The first step in the determination of *Pback* was the calculation of the electric signal belonging to GG: the difference of traces *b* and *a,* i.e., the electric signal due to proton motion [32, 33]. The same type of manipulation with the "GG signals" taken from all data pairs in Fig. 5a–c as in the case of *Mbackelec* resulted in the *Pback* signal as shown also in Fig. 6. The GG signal *c* called *Pforward* corresponds to release of protons from the ground state for blue excitation [32, 33].

Measurements and evaluations were performed at four temperatures. The *Pforward*, *Mbackelec* and *Pback* traces were fitted with two exponentials. The Arrhenius parameters calculated from the temperature dependence of the rate constants are shown in Table 2. Note that the amplitudes of the slow negative components are very small (Fig. 6); consequently, the determination of their lifetime values

Table 2 Wild-type bacteriorhodopsin

Signal	ΔH kJ/mol	ΔS kJ/mol deg	τ at 28 °C (μs)
Mback τ_1	17.0 ± 4.5	−0.10 ± 0.01	28
Mback τ_2	16 ± 14	−0.13 ± 0.11	Not reliable
Pforward τ_1	34.5 ± 1.5	−0.051 ± 0.007	36.6
Pforward τ_2	30.3 ± 1.2	−0.089 ± 0.006	171
Pback τ_1	22.4 ± 1.7	−0.089 ± 0.006	28
Pback τ_2	35.5 ± 2.3	−0.06 ± 0.01	173

Arrhenius parameters of electric signals from averages of three series (partially): *Mback* blue excitation (406 nm) with double laser flashes, *Pforward* electric signal of glycyl-glycine (*GG*), P*back* electric signal of GG for blue flash. Temperature range: 7–28 °C. M concentration was about 25%, and correction for ground state contribution about 50%. Sample absorbance at 570 nm was 0.3. Bathing solution: 50 μM $CaCl_2$, 5 mM GG. For the measurements without GG, an additional 1 mM NaCl was added

involved large error, which is reflected in the Arrhenius parameters.

3.2 Mutant D96N

Because of the lack of the proton donor amino acid, Asp96, the lifetime of the M intermediate for mutant D96N is large, and a quasi-continuous illumination could produce substantial M_{CC} (about 70%) determined from the absorption data (trace *a*) in Fig. 7. This fact could be used to get a better signal-to-noise ratio for the traces of the M cycle. The blue flash, as indicated in trace *b*, excited the M intermediate at 20 ms after the illumination. The other procedures were similar to the case of WTbR. Absorption changes (*Mbackopt*) due to excitation of the M

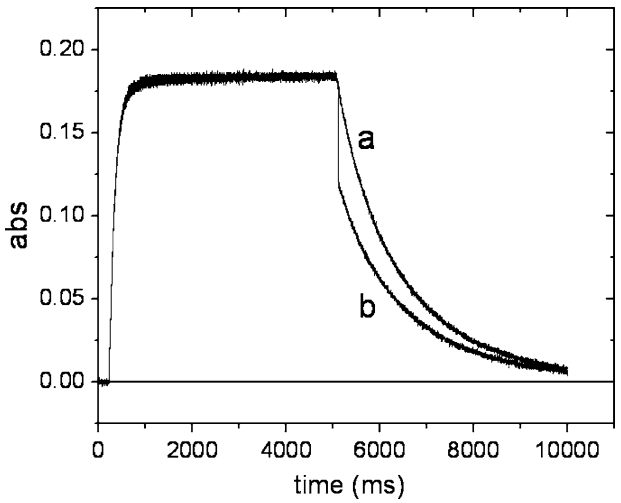

Fig. 7 Mutant D96N. Changes of absorbance at 400 nm for *a* with quasi-continuous illumination for 4 s, *b* the same with blue flash 20 ms after the quasi-continuous illumination. Gel samples, solution 1 mM NaCl, 50 μm $CaCl_2$, temperature 23 °C

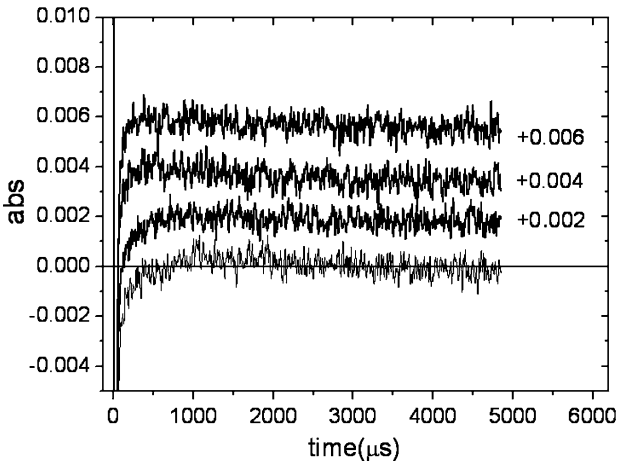

Fig. 8 Mutant D96N. Changes of absorbance at 400 nm connected to the excitation of M intermediate. Traces up–down at 31, 24, 16 and 5 °C, were shifted with the given values. Method of calculation was similar to that in Fig. 3

Table 3 Bacteriorhodopsin mutant D96N Arrhenius parameters of the change in the rise of absorbance, due to excitation of the ground state *Mrise blue* and of M intermediate with blue (406 nm) flash (*Mbackopt*)

Component	ΔH kJ/mol	ΔS kJ/mol deg	τ at 24 °C (μs)
Mriseblue	63.5 ± 2.9	+0.037 ± 0.002	168
Mbackopt	36.6 ± 8.7	−0.049 ± 0.010	98.1

intermediates were determined at a measuring wavelength of 400 nm (Fig. 8). A small negative change appears, the Arrhenius parameters of which are in Table 3 together with those of *Mrise*.

Temperature dependence data for *Mbackopt* in the time range below 6 μs are in [9]. Our measurements covered a much longer time range: the small amplitude rise is seen in Figs. 6 and 7.

Mbackelec, Pforward and *Pback* were determined in a manner similar to the case of WTbR. Figure 9 shows the relevant traces of PERS for the blue flash with and without GG and in the presence or absence of illumination. The advantage of high M_{CC} produced with the background illumination is evident: one sees immediately (i.e., without applying correction for excitation of the residual ground state) that *Mbackelec* and *Pback* contain long-living negative components. The corrections, performed in a manner similar to the case of WTbR, have only a small effect on these traces (compare traces *c* and *d* in Fig. 9 to traces *a* and *b* in Fig. 10), showing also *Pforward* too. We do not emphasize on the deviation of the parameters of *Mbackopt* and *Mbackelec* from each other, as for *Mbackopt* only one lifetime could be fitted and the measurements were performed at one wavelength only. *Pforward* and *Pback* unexpectedly contained three components in the μs

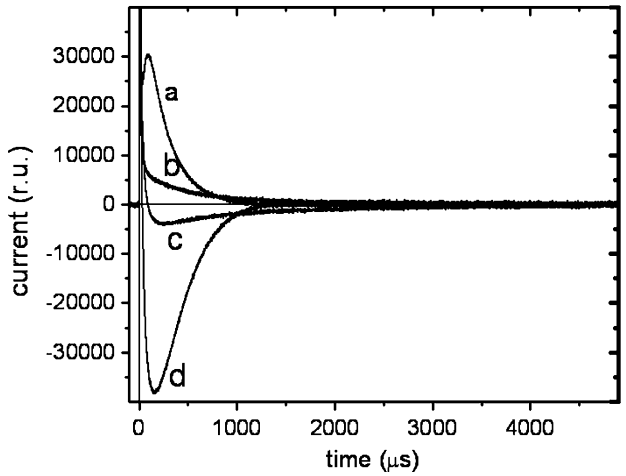

Fig. 9 Mutant D96N. Protein electric response signals *a* with, *b* without glycyl-glycine, both without quasi-continuous illumination, i.e., the BR ground state illuminated with the blue flash, *c* after the quasi-continuous illumination without, and *d* with glycyl-glycine. Gel samples, solution 1 mM NaCl, 50 μm $CaCl_2$, or 50 μm $CaCl_2$ and 5 mM glycyl-glycine, temperature 23 °C

Table 4 Bacteriorhodopsin mutant D96N

Signal	ΔH kJ/mol	ΔS kJ/mol deg	τ at 31 °C (μs)	No. of series
Mback τ_1	14.6 ± 0.8	−0.103 ± 0.006	28.5	5
Mback τ_2	18.9 ± 1.1	−0.12 ± 0.02	521	5
Pforward τ_1	24.5 ± 0.8	−0.076 ± 0.011	24.6	5
Pforward τ_2	32.4 ± 0.1	−0.068 ± 0.002	155	5
Pforward τ_3	62.0 ± 3.0	+0.065 ± 0.003	1,911	2
Pback τ_1	17.1 ± 0.9	−0.089 ± 0.011	97.6	5
Pback τ_2	45.7 ± 1.6	−0.025 ± 0.030	250	5
P back τ_3	33.2 ± 1.0	−0.074 ± 0.014	1,833	2

Arrhenius parameters of electric signals from averages of five series (partially): *Mback* blue excitation (406 nm) after quasi-continuous illumination with yellow light, *Pforward* electric signal of glycyl-glycine (GG) for blue light, *Pback* electric signal of (GG) for blue flash after quasi-continuous illumination with yellow light. Temperature range, 5–30 °C. *M* concentration, about 70%; correction for ground state contribution, about 10%. Sample absorbance at 570 nm 0.3, 50 μM $CaCl_2$, 5 mM Gly-Gly. Without GG, 1 mM NaCl

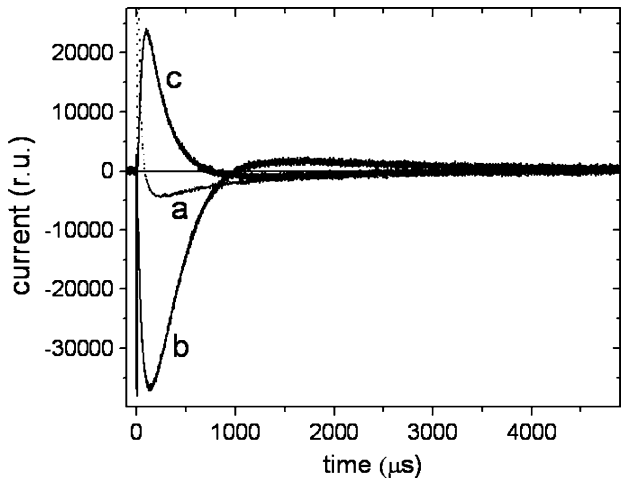

Fig. 10 Mutant D96N. *Mback a* and *Pback b*, signals calculated from traces in Fig. 7, *c Pforward* signal for blue flash

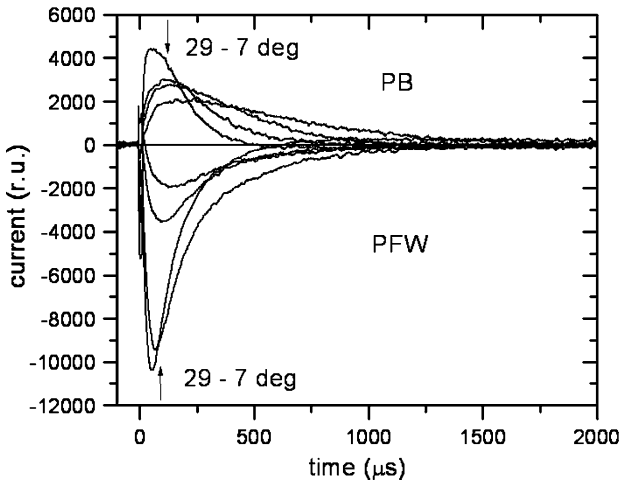

Fig. 11 Mutant D96N. Temperature dependence of *Pforward* (*PFW*) and *Pback* (*PB*) signals calculated from measurements similar to those in Fig. 8, but with 1 mM bis–tris propane (*BTP*) instead of glycyl-glycine. Temperatures: 7, 15, 23 and 29 °C

domain. Unexpectedly, as in the case of WTbR, such a phenomenon did not occur, and the rise in time of proton release, measured separately with the dye pyranine (not shown), coincides with the lifetime of the longer living negative component in *Pforward*. The sign change of the GG signal definitely shows that the direction of proton motion changes during proton release (*Pforward*) and back-take (*Pback*). We assign the appearance of the extra component in *Pforward* and *Pback* to the formation of a ground state-like intermediate in the D96N photocycle, described in [35, 36].

As in the case of WTbR temperature dependence, *Mbackelec* was fitted with two exponentials, while the *Pforward* and *Pback* signals with three exponentials. The corresponding Arrhenius parameters are listed in Table 4.

In our former papers, we have shown that by adding BTP, instead of GG, the buffer signal changes its sign from positive to negative [32, 33]; thus, *Pforward* should turn to negative and *Pback* to positive. The temperature dependence of this phenomenon is shown for mutant D96N in Fig. 11. The BTP signals are smaller than the GG signal by about a factor of 2; nevertheless, the three μs components of *Pforward* and *Pback* are observable. The Arrhenius parameters are similar to the ones in Table 4.

4 Discussion

In this study, we obtained data on the molecular rearrangements of the excitation of the M intermediate of bR. The investigations involved optical and electric phenomena on proton release and back-take processes. The activation parameters (ΔH and ΔS values) of the component signals obtained from temperature dependence measurements, as well as the other results, are expected to be utilized in molecular dynamics simulations of proton transfer steps not yet covered by theoretical model calculations. Conversely, molecular dynamics modeling of the M cycle is expected to unravel the fine details of intramolecular events associated with the experimental data.

In the optical section, negative absorption changes attributed to the excitation of M intermediate (*Mbackopt*) were registered at 400 nm. Though the traces were somewhat noisy (Figs. 2, 7), well-articulated temperature dependences could be established, which allowed us to determine the Arrhenius parameters (see Arrhenius parameters in Tables 1 and 3 together with the parameters of *Mrise*). Note the important differences in the forward and backward direction: the large ΔH values for *Mrise* compared to those for *Mbackopt* and the different sign for ΔS. These dissimilarities clearly indicate that the molecular events involved in these transitions differ: the positive ΔS value points to disorder, while the negative to order when establishing the new intermediate.

The Arrhenius parameters of *Pforward* are in good accordance with those already published for green light excitation of both bR variants [32, 33]. The small deviations may be due to the different excitation (see, e.g., [37]). The lifetimes of the slowest components of *Pforward* and *Pback* coincide with the lifetimes of the proton release and back-take obtained from measurements with proton indicator dyes.

The parameters of the slower (rate-limiting) components of *Mbackelec* and *Pback* were very different in D96N where more reliable signals could be detected. This clearly shows that the actual proton back-take process (represented by slowest component of *Pback*) is preceded by intramolecular charge rearrangements due to a conformational change (represented by *Mbackelec*).

This strongly supports the concept suggested in [32], namely that conformational changes (including electric charge rearrangements) in the protein trigger the proton release in the photocycle of the excited ground state. While, however, clear distinction of the two events in the forward direction is not possible due to kinetic reasons, in the backward process they get naturally separated. It is plausible to assume that the conformational rearrangement in the PRG represented by the *Mbackelec* signal is a sort of reversal of the one that takes place in the forward direction (note that in both cases, a conformational change triggers a proton transfer step). Given this assumption, we can also make interesting conclusions on the normal pumping process.

As mentioned earlier, usually two M intermediates (M_1 with protonated and M_2 with deprotonated protein) are distinguished [38]. In X-ray-based structural models for M_2, the amino acid group Arg82 points toward the cytoplasmic side. Our measurements require the assumption of another intermediate between M_1 and M_2, namely M_1'. Though M_1' was not yet deprotonated, the outward flip of Arg82 and probably the perturbation of several water molecules [20]) had already taken place. Such an intermediate has been predicted in [38]. With the new intermediate, the chronology of the first half of the forward photocycle can be described by the following scheme:

$$\mathrm{BR}-\mathrm{K}-\mathrm{L}-\mathrm{M}_1-\mathrm{M}_1'-\mathrm{M}_2 \qquad (2)$$

The first transition of the scheme is known to be dominated by a *trans–cis* isomerization of the retinal molecule, accompanying the turn of the Schiff-base proton from one side of the molecular axis of retinal to the other. If, for the sake of simplicity, we consider this formally as a proton translocation step, we see that (2) describes a series of alternating proton translocation/transfer and protein conformational change reactions. The chronology in (2) defines also the causality: conformational change ("conf") and proton transfer ("prot") steps trigger, in turn, each other, as a domino effect. Whether such a "domino model" can be extended to the whole photocycle is an open question, but the experimental evidence for the so-called M_N form in the D96N photocycle [39] (an intermediate with a protein conformation similar to that of N, but still with deprotonated Schiff base) is in favor of, at least, the following extension of (2):

$$\begin{array}{l}\mathrm{BR}-\mathrm{K}-\mathrm{L}-\mathrm{M}_1-\mathrm{M}_1'-\mathrm{M}_2-\mathrm{M}_\mathrm{N}-\mathrm{N} \\ \quad \mathrm{prot}\ \mathrm{conf}\ \mathrm{prot}\ \mathrm{conf}\ \mathrm{prot}\ \mathrm{conf}\ \mathrm{prot}\end{array} \qquad (3)$$

In other words, the energy stored by the protein after light excitation is dissipated via a conformational relaxation series mediated by subsequent proton transfer steps. This picture is not in conflict with previous attempts to model the bR photocycle on a didactic basis (the so-called "IST-" and "local access" models) [40, 41]. However, unlike these models, we do not want to explain here the vectorial quality of the proton pump, only to establish a formal rule to assist conceptual understanding of the bR proton pump mechanism. We expect that, given its simplicity, the domino model may turn out to be of more general nature and can be also applied to the functional description of other charge transfer proteins (see supportive theoretical considerations for electron/atom transfer proteins in [42]).

Acknowledgments Discussions with Prof. Sándor Suhai on the general aspects of the bacteriorhodopsin proton pump mechanism are gratefully acknowledged. The research was supported by the Hungarian National Science Fund (OTKA T-049489 and CK 78367). S.G.T. is a visiting professor at the University of the Basque Country and an associate member of the Institute of Biophysics Bulgarian Academy of Sciences.

References

1. Stoeckenius W (1999) Protein Sci 8:447
2. Lanyi JK (2000) Biochim Biophys Acta 1460:1
3. Balashov SP (1995) Israel J Chem 35:415
4. Hessling B, Herbst J, Rammelsberg R, Gerwert K (1997) Biophys J 73:2071
5. Dér A, Keszthelyi L (2001) Biochemistry (Moscow) 66:1234
6. Karvaly B, Dancsházy Zs (1977) FEBS Lett 76:36
7. Ormos P, Dancsházy Zs, Keszthelyi L (1980) Biophys J 31:207
8. Dickopf S, Heyn MP (1997) Biophys J 73:3171
9. Ludmann K, Ganea C, Váró G (1999) J Photochem Photobiol B 49:23
10. Ormos P, Reinisch L, Keszthelyi L (1983) Biochim Biophys Acta 722:471
11. Trissl HW, Gärtner W, Leibl W (1989) Chem Phys Lett 158:515
12. Tóth-Boconádi R, Dér A, Taneva SG, Keszthelyi L (2006) Biophys J 90:2651
13. Tóth-Boconádi R, Taneva SG, Keszthelyi L (2001) J Biol Phys Chem 1:58
14. Luecke H, Schobert B, Richter HT, Cartailler JP, Lanyi JK (1999) Science 286:255
15. Hayashi S, Tajkhorshid E, Schulten K (2002) Biophys J 83:1281
16. Murata K, Fuji Y, Nobuyuki E, Hata M, Hoshino T, Tsuda M (2000) Biophys J 79:982
17. Bondar A-N, Suhai S, Fischer S, Smith JC, Elstner M (2007) J Struct Biol 157:454
18. Song Y, Mao J, Gunner MR (2003) Biochemistry 42:9875
19. Rousseau R, Kleinschidt W, Schmitt UW, Marx D (2004) Angew Chem Int Ed 43:4804
20. Garczarek F, Gerwert K (2006) Nature 439:109
21. Phatak P, Ghosh N, Yu H, Cui Q, Elstner M (2009) Proc Natl Acad Sci USA 105:19672
22. Dér A, Oroszi L, Kulcsár Á, Zimányi L, Tóth-Boconádi R, Keszthelyi L, Stoeckenius W, Ormos P (1999) Proc Natl Acad Sci USA 96:2776
23. Royant A, Edman K, Ursby T, Pebay-Peyroula E, Landau EM, Neutze R (2000) Nature 406:645
24. Lanyi JK, Schobert B (2003) J Mol Biol 328:439
25. Kouyama T, Nishikawa T, Tokuhisa T, Okamura H (2004) J Mol Biol 335:469
26. Edman K, Royant A, Larsson G, Jacobson F, Taylor T, Van Der EM, Landau EM, Pebay-Peyroula E, Neutze R (2004) J Biol Chem 279:2147
27. Sass HJ, Büldt G, Gessenich R, Hehn D, Neff D, Schlesinger R, Berendzen J, Ormos P (2000) Nature 406:649
28. Tóth-Boconádi R, Dér A, Fábián L, Taneva SG, Keszthelyi L (2009) Photochem Photobiol 85:609
29. Tóth-Boconádi R, Taneva SG, Fábián L, Dér A, Keszthelyi L (2007) J Biol Phys Chem 7:147
30. Dér A, Hargittai P, Simon J (1985) J Biochem Biophys Methods 10:295
31. Zimányi L, Saltiel J, Brown LS, Lanyi JK (2006) J Phys Chem A 110:2318
32. Tóth-Boconádi R, Dér A, Keszthelyi L (2000) Biophys J 78:3170
33. Tóth-Boconádi R, Dér A, Taneva SG, Tuparev N, Keszthelyi L (2001) Eur Biophys J 30:140
34. Porschke D (2002) J. Phys. Chem. B. 106:10233
35. Zimányi L, Kulcsár A, Lanyi JK, Sears DP, Saltiel J (1999) Proc Natl Acad Sci USA 96:4414
36. Tóth-Boconádi R, Taneva SG, Keszthelyi L (2001) J Photochem Photobiol B 65:122
37. Tóth-Boconádi R, Taneva SG, Keszthelyi L (2005) Biophys J 89:2605
38. Zimányi L, Váró G, Chang M, Ni BF, Needleman R, Lanyi JK (1992) Biochemistry 31:8535
39. Sasaki J, Shichida Y, Lanyi JK, Maeda A (1992) J Biol Chem 267:20782
40. Haupts U, Tittor J, Bamberg E, Oesterhelt D (1997) Biochemistry 36:2
41. Lanyi JK (1998) Biochim Biophys Acta 1365:17
42. Dogonadze RR, Kuznetzov AM, Ulstrup J (1977) J Theor Biol 69:239